Accepted Manuscript

(*E*)-1,3-diphenyl-1*H*-pyrazole derivatives containing O-benzyl oxime moiety as potential immunosuppressive agents: Design, synthesis, molecular docking and biological evaluation

Xian-Hai Lv, Qing-Shan Li, Zi-Li Ren, Ming-Jie Chu, Jian Sun, Xin Zhang, Man Xing, Hai-Liang Zhu, Hai-Qun Cao

PII: S0223-5234(15)30406-2

DOI: 10.1016/j.ejmech.2015.12.020

Reference: EJMECH 8260

To appear in: *European Journal of Medicinal Chemistry*

Received Date: 19 June 2015

Revised Date: 1 December 2015

Accepted Date: 10 December 2015

Please cite this article as: X.-H. Lv, Q.-S. Li, Z.-L. Ren, M.-J. Chu, J. Sun, X. Zhang, M. Xing, H.-L. Zhu, H.-Q. Cao, (*E*)-1,3-diphenyl-1*H*-pyrazole derivatives containing O-benzyl oxime moiety as potential immunosuppressive agents: Design, synthesis, molecular docking and biological evaluation, *European Journal of Medicinal Chemistry* (2016), doi: 10.1016/j.ejmech.2015.12.020.

(*E*)-1,3-diphenyl-1*H*-pyrazole derivatives containing O-benzyl oxime moiety as potential immunosuppressive agents: Design, synthesis, molecular docking and biological evaluation

Xian-Hai Lv [a], Qing-Shan Li [b], Zi-Li Ren [a], Ming-Jie Chu [a], Jian Sun [c], Xin Zhang [c], Man Xing [c], Hai-Liang Zhu*[c], Hai-Qun Cao*[a]

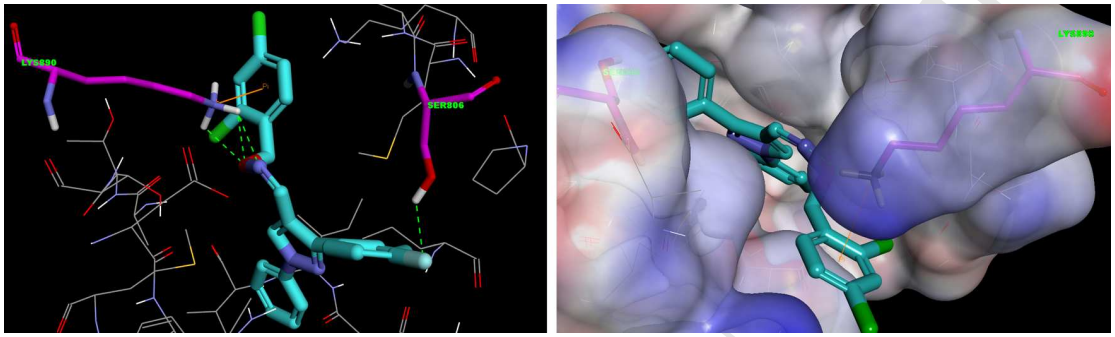

A series of novel pyrazole derivatives containing *O*-benzyl oxime moiety were reported in this study for their significantly immunosuppressive activities. Compound **4n** exhibited the most potent inhibitory activity (IC_{50}=1.18 μM for lymph node cells and IC_{50} = 0.28 μM for PI3Kγ).

(*E*)-1,3-diphenyl-1*H*-pyrazole derivatives containing O-benzyl oxime moiety as potential immunosuppressive agents: Design, synthesis, molecular docking and biological evaluation

Xian-Hai Lv [a], Qing-Shan Li [b], Zi-Li Ren [a], Ming-Jie Chu [a], Jian Sun [c], Xin Zhang [c], Man Xing [c], Hai-Liang Zhu*[c], Hai-Qun Cao*[a]

[a]*College of Plant Protection, Anhui Agricultural University, Hefei 230036, P.R. China*

[b]*School of Medical Engineering, Hefei University of Technology, Hefei 230009, P.R. China*

[c]*State Key Laboratory of Pharmaceutical Biotechnology, Nanjing University, Nanjing 210093, P.R. China*

Abstract: A series of novel (*E*)-1,3-diphenyl-1*H*-pyrazole derivatives containing O-benzyl oxime moiety were firstly synthesized and their immunosuppressive activities were evaluated. Among all the compounds, **4n** exhibited the most potent inhibitory activity (IC_{50}=1.18 μM for lymph node cells and IC_{50} = 0.28 μM for PI3Kγ), which was comparable to that of positive control. Moreover, selected compounds were tested for their inhibitory activities against IL-6 released in ConA-simulated mouse lymph node cells, **4n** exhibited the most potent inhibitory ability. Furthermore, in order to study the preliminary mechanism of the compounds with potent inhibitory activity, the RT-PCR experiment was performed to assay the effect of selected compounds on mRNA expression of IL-6. Among them, compound **4n** strongly inhibited the expression of IL-6 mRNA.

Keywords: Immunosuppressant; Molecular docking; Oxime ethers; PI3Kγ; Pyrazole.

---

* Corresponding author. Tel. & fax: +86 551 65786906, E-mail: haiquncao@163.com

Abbreviations: PI3K, Phosphoinositide 3-kinase; IL-6, interleukin-6; AKT, protein kinase B; NaOAc, CH_3COONa; CsA, cyclosporin A; ConA, Concanavalin A; SAR,

structure–activity relationships; CADD, computer assistant drug design; SI, selective index, CC_{50}/IC_{50}; mp, melting point; DMF, N,N-Dimethylformamide.

1. Introduction

Immunosuppressant has been one of the most prescribed drugs in the world, widely used in the treatment of autoimmune diseases, including rheumatoid arthritis, systemic lupus erythematosus, multiple sclerosis, type I diabetes mellitus, psoriasis, and inflammatory bowel disease[1]. Although immunosuppressive drugs have been used for the clinical treatment of autoimmune diseases, their side effects including liver toxicity, nephro toxicity, infection, cardiovascular toxicity and others which limit their clinical applications[2-4]. Thus, there is an urgent need for the design and development of novel and less toxic anti-inflammatory agents.

Phosphoinositide 3-kinases (PI3Ks) phosphorylate the 3-hydroxyl of the head group of phosphatidylinositol (PtdIns), and of phosphorylated derivatives of PtdIns termed phosphoinositides[5]. PI3Ks are key components of the PI3K/AKT pathway which plays essential roles in various cellular activities including cell proliferation, cell survival, membrane trafficking, glucose transport, neurite outgrowth, membrane ruffling, superoxide production[6, 7]. The dysregulation of the PI3K pathway is associated with numerous cancers as well as inflammatory and autoimmune diseases[8, 9]. PI3Ks are grouped into three classes (I, II, and III) according to their structure preference and substrate specificity, class I PI3Ks are separated into two subfamilies (IA and IB) depending on the receptors to which they couple[9-11]. Among these isoforms, PI3Kγ (the only isoform of class IB) plays a pivotal role in inflammation, and it is involved in allergy, development of chronic inflammation, autoimmune diseases[12, 13]. Therefore, there is important significance to discover new agents that can influence PI3Kγ.

Figure 1.

The oxime ether moiety have received significant attention for this structural scaffold makes up the core structure of numerous biologically active compounds in chemical, food and pharmaceutical research. Some oxime-ether derivatives of hydroxylated benzaldehydes and acetophenones were found to possess pronounced nonsteroidal anti-inflammatory activities and favorable toxicities.[14-18]. On the

other hand, it was found that a number of other 1,3-substituted 1*H*-pyrazole derivatives (Figure 1. A, B and C) showed potent anti-inflammatory activity[19-21]. In continuation of our research work on the development of new anti-inflammatory agents[22-24], we report the design and SAR of a series of novel (*E*)-1,3-diphenyl-1*H*-pyrazole oxime ether derivatives (Figure 2) in this study. Introducing the oxime ether moiety into the 1,3-substituted 1*H*-pyrazole skeleton leads to a positive result in preliminary *in silico* screening. The binding model generated by molecular modeling process revealed that the designed (*E*)-1,3-diphenyl-1*H*-pyrazole oxime ether derivative was tightly embedded in the binding sites of PI3Kγ via hydrogen bonds and π–cation interactions (Figure 3).

Figure 2.

Figure 3.

2. Results and discussion

2.1 Chemistry

Twenty (*E*)-1,3-diphenyl-1*H*-pyrazole-4-carbaldehyde O-benzyl oxime derivatives (**4a–4t**) were firstly synthesized and the general pathway outlined in Scheme 1. The requisite intermediates **3** and **4** were prepared by the reaction of the Vilsmeier–Haack reagent (DMF/$POCl_3$) and phenyl hydrazones **1** and **2,** respectively[25]. Then target compounds **4a–4t** were synthesized by direct addition-elimination reactions of 1.0 equivalent of corresponding intermediates **3**/**4** and 1.2 equivalents of O-benzylhydroxylamine hydrochloride in the presence of NaOAc as catalytic agent. Then compounds **4a–4t** were obtained by subsequent purification with recrystallisation in methanol. All of the synthetic compounds gave satisfactory analytical and spectroscopic data, which were in full accordance with their depicted structures. Compound **4m** was successfully crystallized and its structure was determined by single-crystal X-ray diffraction analysis. The structure was solved by direct methods and refined on F^2 by full-matrix least-squares methods using SHELXL-97[26]. The crystal data, data collection, and refinement parameter for the

compound **4m** are listed in Table 1, the crystal structure is shown in Figure 4.

Scheme 1

Table 1

Figure 4

2.2 Cytotoxicity and inhibitory activity

The inhibitory activity of tested compound is sometimes a result of their toxic effect and consequently might cause an erroneous conclusion, so we performed cytotoxicity test before inhibitory activity assay of target compounds. (*E*)-1,3-diphenyl-1*H*-pyrazole oxime ether derivatives **4a–4t** were screened for their cyotoxicities on lymph node cells with cyclosporin A (CsA) as the positive control, the cytotoxicity of each compound was expressed as the CC_{50} values which were summarized in Table 2. The results depicted that most of the compounds were low toxic.

Table 2

T cells play a pivotal role in immune response. Excessive T-cell proliferation and activation has been implicated in the pathogenesis of a variety of inflammatory diseases. Next, all the synthetic (*E*)-1,3-diphenyl-1*H*-pyrazole oxime ether derivatives **4a–4t** were tested for evaluated for their *in vitro* inhibitory activity on murine lymphocyte proliferation induced by Concanavalin A (ConA). The immunosuppressive activity of each compound was expressed as the concentration of the compound that inhibited ConA stimulated T cells proliferation to 50 % (IC_{50}) of the control value, and the results were summarized in Table 2. In general, it was observed that a number of synthesized pyrazole oxime ether analogues displayed potent immunosuppressive activities in the low micromolar range. Inspection of the chemical structure of the compounds **4a–4t** suggested that it could be divided into two subunits: A and B rings. A comparison of the *para* substituents on the A-ring demonstrated that an electron-withdrawing group have improved immunosuppressive activity and the potency order is F > Cl > OMe >H > Me. SAR also suggested that compounds bearing the same substituents on phenyl ring A exhibited distinct

inhibitory activity due to the difference of the substituents on the ring B. Among these compounds, compounds with *ortho* electron-withdrawing substitution (**4m**-**4t**) showed stronger anti-inflammatory activities in the following order: F > Cl > H. Furthermore, introduction of substituent to *para*-position of ring B results in less active analog (**4d**, **4h**, **4p** and **4t**). Among all the compounds, **4n** and **4o** exhibited the most potent inhibitory activities (2.16 and 1.74 μM, respectively), which owing *para*-F group in the A ring and *para*-F/2,4-Cl in the B ring. Furthermore, the cytotoxicity and SI of the compound **4n** (SI=219.59) and **4o** (SI=108.35) have absolute advantage compared to others, which demonstrated that these compounds could selectively inhibited the proliferation of ConA stimulated T cells. Considering the high inhibitory potency and low toxicity, it can be concluded that compound **4n** and **4o** could be potential anti-inflammatory agents.

2.3 PI3Kγ enzymatic activity

Based on the data of cellular immunosuppressive activities obtained before, the top 7 compounds (**4n**, **4p**, **4o**, **4r**, **4s**, **4b** and **4t**) and the bottom 3 compounds (**4g**, **4h** and **4e**) were selected for evaluate their PI3Kγ inhibitory activities compared with LY294002[27]. The results were summarized in Table 3. Among the tested compounds, **4n** showed the most potent inhibitory activity with IC_{50} of 0.28 μM, which was comparable to the positive control LY294002 with IC_{50} of 7.2 μM. As shown in Table 3, for tested pyrazole oxime ether derivatives, the SAR of PI3Kγ inhibitory activities were consistent with their inhibitory activities of ConA stimulated T cells proliferation, all the bottom compounds showed poor PI3Kγ inhibitory activities while most of the top compounds displayed potent inhibitory activities. The results indicated that the potent anti-inflammatory activities of the synthetic compounds were probably correlated to their PI3Kγ inhibitory activities.

2.4 IL-6 inhibitory activity

IL-6 (interleukin-6), is an important multifunctional pro-inflammatory cytokine, contributes to the initiation and extension of the inflammatory process and considered

as a central mediator in a range of inflammatory diseases[28-30]. It has been found that the activation of PI3K signaling pathway leading to up-regulation of IL-6 expression[31].

To determine whether target compounds suppress activation of AKT (a key downstream effector of PI3K and important node in the PI3K/AKT signaling pathway), selected compounds **4n**, **4o**, **4p** and **4r** were tested for their inhibitory activities against IL-6 released in ConA-simulated mouse lymph node cells. As shown in Figure 5.A, among these seven compounds, **4n** exhibited the highest inhibitory effect against ConA-induced IL-6 expression. Furthermore, in order to study the preliminary mechanism of the compounds with potent inhibitory activity, the RT-PCR experiment was performed to assay the effect of four selected compounds on mRNA expression of IL-6. The RT-PCR results were summarized in Figure 5.B. Among them, compound **4n** strongly inhibited the expression of IL-6 mRNA. Combining with the results of PI3Kγ inhibitory activity assay, it can be inferred that compound **4n** might inhibit IL-6 production through blocking activation of PI3K/AKT signaling pathway.

3. Conclusions

In conclusion, a series of pyrazole derivatives containing *O*-benzyl oxime moiety were firstly synthesized and evaluated for their immunosuppressive activity. It is worth noticing that compound **4n** demonstrated the most outstanding immunosuppressive effect in vitro with IC_{50} of 1.18 μM which was comparable to that of cyclosporin A (IC_{50}= 0.57μM). Meanwhile, compounds **4n**, **4p**, **4o** and **4r** that exhibited significant immunosuppressive activities were evaluated for their PI3Kγ inhibitory activities. The results showed that compound **4n** displayed the most potent inhibitory activity (IC_{50} = 0.28 μM), which was more potent than that of LY294002. Moreover, compounds **4n**, **4p**, **4o** and **4r** were assayed for PI3K/AKT signaling pathway inhibition using the ELISA assay. We examined the compounds with potent inhibitory activities against IL-6 released in ConA-simulated mouse lymph node cells. **4n** exhibited the highest inhibitory effect against ConA-induced IL-6 expression.

Furthermore, in order to study the preliminary mechanism of the compounds with potent inhibitory activity, the RT-PCR experiment was performed to assay the effect of **4n**, **4p**, **4o** and **4r** on mRNA expression of IL-6.The results showed that the apoptosis induced by 4p might be mediated by the inhibition of PI3K/AKT signaling pathway. Molecular docking study indicated that compound **4n** was nicely bound to the PI3Kγ with two hydrogen bonds. All the results showed the great potential of compound **4n** as an immunosuppressant targeting PI3Kγ.

Acknowledgement

This work was supported by National Natural Science Foundation of China (No.21302002) and Anhui Provincial Natural Science Foundation (1408085QB33, 1508085MB33).

4. Experimental section

4.1. General

All of the synthesized compounds were chemically characterized by thin layer chromatography (TLC), proton nuclear magnetic resonance (^{1}H NMR) and elemental microanalyses (CHN). ^{1}H NMR spectra were measured on a Bruker AV-300 or a Agilent DD2 600Hz spectrometer at 25 ^{o}C. Chemical shifts were reported in ppm (δ) using the residual solvent line as internal standard and referenced to Me_4Si. Splitting patterns were designed as s, singlet; d, doublet; t, triplet; m, multiplet. ESI-MS spectra were recorded on a Mariner System 5304 Mass spectrometer. Elemental analyses were performed on a CHN-O-Rapid instrument and were within ±0.4% of the theoretical values. Melting points were determined on a XT4 MP apparatus (Taike Corp., Beijing, China) and were as read. Analytic thin-layer chromatography was performed on the glass backed silica gel sheets (silica gel 60 A GF254). All compounds were detected using UV light (254 nm or 365 nm).

4.2. General method for the preparation of target compounds 3a-3e

The starting material 1,3-diphenyl-1H-pyrazole-4-carbaldehyde **(3a-3e)** were

synthesized as following: para-substituted acetophenone (**1a-1e**) (20 mmol) interact with phenylhydrazine hydrochloride (25 mmol) couple with sodium acetate (40 mmol) in anhydrous ethanol to form 1-phenyl-2-(1- phenylethylidene) hydrazine (**2a-2e**), which was then dissolved in a cold mixed solution of DMF (20 mL) and $POCl_3$ (16 mL), stirred at 50-60 ^oC for 5 h. The resulting mixture was poured into ice-cold water, a saturated solution of sodium hydroxide was added to neutralize the mixture, and the solid precipitate was filtered, washed with water, dried and recrystallized from ethanol to give the compounds **3a-3e**.

4.3. General procedure for (*E*)-1,3-diphenyl-1*H*-pyrazole-4-carbaldehyde *O*-benzyl oxime derivatives 4a-4t

To a solution of **3a-3e** (1 mmol) in anhydrous ethanol (10 mL), corresponding *O*-benzylhydroxylamine hydrochloride (1 mmol) and NaOAc (1.2 mmol) were added and the resulting solution was stirred at the room temperate for 3 h. The mixture was concentrated and taken in ethyl acetate (20 mL), washed with water (20 mL), saturated sodium chloride solution (20 mL) and dried over sodium sulfate. The resulting solution was concentrated and the purification of the residue by recrystallization from ethanol yielded the desired compounds **4a–4t**.

*4.3.1 (E)-1,3-diphenyl-1H-pyrazole-4-carbaldehyde O-benzyl oxime (**4a**)*

White solid, yield: 80%. Mp: 73-75 ^oC. ^1H NMR (300 MHz, $CDCl_3$): 5.34 (s, 2H); 7.30-7.53 (m, 11H); 7.66 (d, *J*=6.39Hz, 2H); 7.78 (d, *J*=7.83Hz, 2H); 8.36 (s, 1H); 8.84 (s, 1H). MS (ESI): 354.5 ($C_{23}H_{19}N_3O$, $[M+H]^+$). Anal. Calcd for $C_{23}H_{19}N_3O$: C, 78.16; H, 5.42; N, 11.89; Found: C, 78.18; H, 5.46; N, 11.92%.

*4.3.2 (E)-1,3-diphenyl-1H-pyrazole-4-carbaldehyde O-(2-fluorobenzyl) oxime (**4b**)*

White solid, yield: 73%. Mp: 55-57 ^oC. ^1H NMR (300 MHz, $CDCl_3$): 5.40 (s, 2H); 7.15 (m, 1H);7.31-7.52 (m, 9H); 7.65 (d, *J*=7.68Hz, 2H); 7.76 (d, *J*=7.68Hz, 2H); 8.35 (s, 1H); 8.86 (s, 1H). MS (ESI): 372.8 ($C_{23}H_{18}FN_3O$, $[M+H]^+$). Anal. Calcd for $C_{23}H_{18}FN_3O$: C, 74.42; H, 4.83; N, 11.40; Found: C, 74.38; H, 4.88; N, 11.31%.

*4.3.3 (E)-1,3-diphenyl-1H-pyrazole-4-carbaldehyde O-(2-chlorobenzyl) oxime (**4c**)*

White solid, yield: 80%. Mp: 74-76 ^{o}C. ^{1}H NMR (300 MHz, $CDCl_3$): 5.45 (s, 2H); 7.27 (m, 1H);7.33-7.53 (m, 9H); 7.66 (d, *J*=6.39Hz, 2H); 7.78 (d, *J*=7.50Hz, 2H); 8.36 (s, 1H); 8.93 (s, 1H). MS (ESI): 388.9 ($C_{23}H_{18}ClN_3O$, $[M+H]^+$). Anal. Calcd for $C_{23}H_{18}ClN_3O$: C, 71.22; H, 4.68; N, 10.83; Found: C, 72.35; H, 4.72; N, 10.96%.

*4.3.4 (E)-1,3-diphenyl-1H-pyrazole-4-carbaldehyde O-(2,4-dichlorobenzyl) oxime (**4d**)*

White solid. Yield: 87%. Mp: 103-104 ^{o}C. ^{1}H NMR (300 MHz, $CDCl_3$): 5.40 (s, 2H); 7.24 (d, *J*=2.01Hz, 1H);7.28-7.52 (m, 8H); 7.65 (d, *J*=6.42Hz, 2H); 7.77 (d, *J*=7.68Hz, 2H); 8.34 (s, 1H); 8.91 (s, 1H). MS (ESI): 422.7 ($C_{23}H_{17}Cl_2N_3O$, $[M+H]^+$). Anal. Calcd for ($C_{23}H_{17}Cl_2N_3O$: C, 65.41; H, 4.06; N, 9.95; Found: C, 65.57; H, 4.12; N, 10.03%.

*4.3.5 (E)-1-phenyl-3-(p-tolyl)-1H-pyrazole-4-carbaldehyde O-benzyl oxime (**4e**)*

White solid. Yield: 79%. Mp: 70-72 ^{o}C. ^{1}H NMR (300 MHz, $CDCl_3$): 2.42 (s, 3H); 5.34 (s, 2H); 7.27-7.57 (m, 10H); 7.73 (d, *J*=8.25Hz, 2H); 7.78 (d, *J*=8.04Hz, 2H); 8.35 (s, 1H); 8.83 (s, 1H). MS (ESI): 368.3 ($C_{24}H_{21}N_3O$, $[M+H]^+$). Anal. Calcd for $C_{24}H_{21}N_3O$: C, 78.45; H, 5.76; N, 11.44; Found: C, 78.55; H, 5.77; N, 11.56%.

*4.3.6 (E)-1-phenyl-3-(p-tolyl)-1H-pyrazole-4-carbaldehyde O-(2-fluorobenzyl) oxime (**4f**)*

White solid. Yield: 69%. Mp: 40-42 ^{o}C. ^{1}H NMR (300 MHz, $CDCl_3$): 2.47 (s, 3H); 5.19 (s, 2H); 7.23 (m, 1H);7.30-7.60 (m, 8H); 7.88 (d, *J*=8.40Hz, 2H); 7.94 (d, *J*=8.40Hz, 2H); 8.26 (s, 1H); 8.90 (s, 1H). MS (ESI): 386.9 ($C_{24}H_{20}FN_3O$, $[M+H]^+$). Anal. Calcd for $C_{24}H_{20}FN_3O$: C, 74.79; H, 5.23; N, 10.90; Found: C, 74.84; H, 5.00; N, 11.15 %.

*4.3.7 (E)-1-phenyl-3-(p-tolyl)-1H-pyrazole-4-carbaldehyde O-(2-chlorobenzyl) oxime (**4g**)*

White solid. Yield: 79%. Mp: 56-58 °C. ^{1}H NMR (300 MHz, DMSO-d_6): 2.48 (s, 3H); 5.24 (s, 2H); 7.28 (m, 1H); 7.30-7.61 (m, 8H); 7.89 (d, *J*=8.22Hz, 2H); 7.95 (d, *J*=8.22Hz, 2H); 8.32 (s, 1H); 8.87 (s, 1H). MS (ESI): 403.0 ($C_{24}H_{20}ClN_3O$, $[M+H]^+$). Anal. Calcd for $C_{24}H_{20}ClN_3O$: C, 71.73; H, 5.02; N, 10.46; Found: C, 71.82; H, 4.98; N, 10.62%.

*4.3.8 (E)-1-phenyl-3-(p-tolyl)-1H-pyrazole-4-carbaldehyde O-(2,4-dichlorobenzyl) oxime (**4h**)*

White solid. Yield: 85%. Mp: 103-104 °C. ^{1}H NMR (300 MHz, $CDCl_3$): 2.42 (s, 3H); 5.39 (s, 2H); 7.25 (d, *J*=2.02Hz, 1H);7.27-7.52 (m, 7H); 7.55 (d, *J*=7.68Hz, 2H); 7.77 (d, *J*=7.86Hz, 2H); 8.32 (s, 1H); 8.87 (s, 1H). MS (ESI): 437.2 ($C_{24}H_{19}Cl_2N_3O$, $[M+H]^+$). Anal. Calcd for $C_{24}H_{19}Cl_2N_3O$: C, 66.06; H, 4.39; N, 9.63; Found: C, 66.28; H, 4.19; N, 9.75%.

*4.3.9 (E)-3-(4-methoxyphenyl)-1-phenyl-1H-pyrazole-4-carbaldehyde O-benzyl oxime (**4i**)*

White solid. Yield: 82%. Mp: 78-80 °C. ^{1}H NMR (300 MHz, $CDCl_3$): 3.86 (s, 3H); 5.34 (s, 2H); 6.99 (t, *J*=8.79Hz, 2H); 7.30-7.61 (m, 8H); 7.73 (d, *J*=7.68Hz, 2H); 7.77 (d, *J*=7.89Hz, 2H); 8.35 (s, 1H); 8.82 (s, 1H). MS (ESI): 384.3 ($C_{24}H_{21}N_3O_2$, $[M+H]^+$). Anal. Calcd for $C_{24}H_{21}N_3O_2$: C, 75.18; H, 5.52; N, 10.96; Found: C, 75.33; H, 5.65; N, 11.06%.

*4.3.10 (E)-3-(4-methoxyphenyl)-1-phenyl-1H-pyrazole-4-carbaldehyde O-(2-fluorobenzyl) oxime (**4j**)*

White solid. Yield: 70%. Mp: 88-89 °C. ^{1}H NMR (300 MHz, $CDCl_3$): 3.86 (s, 3H); 5.40 (s, 2H); 6.99 (t, *J*=8.40Hz, 2H); 7.15 (m, 1H);7.32-7.50 (m, 6H); 7.59 (d, *J*=8.61Hz, 2H); 7.75 (d, *J*=7.68Hz, 2H); 8.28 (s, 1H); 8.84 (s, 1H). MS (ESI): 402.7 ($C_{24}H_{20}FN_3O_2$, $[M+H]^+$). Anal. Calcd for $C_{24}H_{20}FN_3O_2$: C, 71.81; H, 5.02; N, 10.47; Found: C, 71.92; H, 5.00; N, 10.63%.

*4.3.11 (E)-3-(4-methoxyphenyl)-1-phenyl-1H-pyrazole-4-carbaldehyde O-(2-chlorobenzyl) oxime (**4k**)*

White solid. Yield: 78%. Mp: 79-81 °C. ^{1}H NMR (300 MHz, $CDCl_3$): 3.87 (s, 3H); 5.44 (s, 2H); 7.02 (t, *J*=8.58Hz, 2H); 7.28 (m, 1H); 7.32-7.47 (m, 6H); 7.67 (d, *J*=8.68Hz, 2H); 7.80 (d, *J*=8.58Hz, 2H); 8.42 (s, 1H); 8.91 (s, 1H). MS (ESI): 418.7 ($C_{24}H_{20}ClN_3O_2$, $[M+H]^+$). Anal. Calcd for $C_{24}H_{20}ClN_3O_2$: C, 68.98; H, 4.82; N, 10.06; Found: C, 69.03; H, 4.78; N, 10.16%.

*4.3.12 (E)-3-(4-methoxyphenyl)-1-phenyl-1H-pyrazole-4-carbaldehyde O-(2,4-dichlorobenzyl) oxime (**4l**)*

White solid. Yield: 87%. Mp: 108-110 °C. ^{1}H NMR (300 MHz, $CDCl_3$): 3.86 (s, 3H); 5.39 (s, 2H); 7.00 (t, *J*=8.76Hz, 2H); 7.27 (m, 1H);7.31-7.50 (m, 5H); 7.59 (d, *J*=7.38Hz, 2H); 7.77 (d, *J*=7.50Hz, 2H); 8.30 (s, 1H); 8.86 (s, 1H). MS (ESI): 452.7 ($C_{24}H_{19}Cl_2N_3O_2$, $[M+H]^+$). Anal. Calcd for $C_{24}H_{19}Cl_2N_3O_2$: C, 63.73; H, 4.23; N, 9.29; Found: C, 63.87; H, 4.09; N, 9.36%.

*4.3.13 (E)-3-(4-fluorophenyl)-1-phenyl-1H-pyrazole-4-carbaldehyde O-benzyl oxime (**4m**)*

Colorless crystal. Yield: 81%. Mp: 73-75 °C. ^{1}H NMR (300 MHz, DMSO-d_6): 5.13 (s, 2H); 7.28 (t, *J*=8.97Hz, 2H); 7.34-7.55 (m, 8H); 7.75 (q, *J*=5.67Hz, 2H); 7.94 (t, *J*=8.04Hz, 2H); 8.28 (s, 1H); 8.88 (s, 1H). ^{13}C NMR (600 MHz, DMSO-d_6):163.51; 161.88;150.47;142.41;139.33;130.88;130.83;130.05;128.77;128.66;128.24;127.45;11 9.64;119.15;115.99;113.82;75.65. The spectra were presented in *supplementary material*. MS (ESI): 372.8 ($C_{23}H_{18}FN_3O$, $[M+H]^+$). Anal. Calcd for $C_{23}H_{18}FN_3O_2$: C, 74.38; H, 4.88; N, 11.31; Found: C, 74.42; H, 4.65; N, 11.46%.

*4.3.14 (E)-3-(4-fluorophenyl)-1-phenyl-1H-pyrazole-4-carbaldehyde O-(2-fluorobenzyl) oxime (**4n**)*

White solid. Yield: 65%. Mp: 89-90 °C. ^{1}H NMR (300 MHz, DMSO-d_6): 5.18 (s, 2H); 7.20 (m, 1H); 7.25 (t, *J*=8.79Hz, 2H); 7.32-7.59(m, 6H); 7.72 (d, *J*=8.68Hz, 2H); 7.94

(d, *J*=7.68Hz, 2H); 8.28 (s, 1H); 8.87 (s, 1H). ^{13}C NMR (600 MHz, DMSO-d_6):163.52;161.89;160.07;150.48;142.75;139.31;131.66;131.63;130.89;130.84;130.69;130.05;128.95;127.47;124.85;119.16;115.97;113.68;69.46. The spectra were presented in *supplementary material*. MS (ESI): 390.7 ($C_{23}H_{17}F_2N_3O$, $[M+H]^+$). Anal. Calcd for $C_{23}H_{17}F_2N_3O$: C, 70.94; H, 4.40; N, 10.79; Found: C, 71.02; H, 4.23; N, 10.83%.

*4.3.15 (E)-3-(4-fluorophenyl)-1-phenyl-1H-pyrazole-4-carbaldehyde O-(2-chlorobenzyl) oxime (**4o**)*

White solid. Yield: 78%. Mp: 75-77 °C. ^{1}H NMR (300 MHz, DMSO-d_6): 5.22 (s, 2H); 7.29 (t, *J*=8.58Hz, 2H); 7.37 (m, 3H); 7.47-7.55 (m, 4H); 7.77 (d, *J*=6.75Hz, 2H); 7.94 (d, *J*=7.47Hz, 2H); 8.33 (s, 1H); 8.88 (s, 1H). ^{13}C NMR (600 MHz, DMSO-d_6): 163.52;161.90;150.54;142.95;139.31;132.88;130.90;130.88;130.85;130.10;130.05;129.71;128.86;127.68;127.47;119.16;116.01;113.63;72.84. The spectra were presented in *supplementary material*. MS (ESI): 406.2 ($C_{23}H_{17}ClFN_3O$, $[M+H]^+$). Anal. Calcd for $C_{23}H_{17}ClFN_3O$: C, 68.07; H, 4.22; N, 10.35; Found: C, 68.14; H, 4.37; N, 10.46%.

*4.3.16 (E)-3-(4-fluorophenyl)-1-phenyl-1H-pyrazole-4-carbaldehyde O-(2,4-dichlorobenzyl) oxime (**4p**)*

White solid. Yield: 81%. Mp: 135-136 °C. ^{1}H NMR (300 MHz, $CDCl_3$): 5.39 (s, 2H); 7.17 (t, *J*=8.58Hz, 2H); 7.27 (m, 1H); 7.35-7.51 (m, 5H); 7.63 (d, *J*=8.61Hz, 2H); 7.76 (d, *J*=7.50Hz, 2H); 8.31 (s, 1H); 8.87 (s, 1H). MS (ESI): 441.9 ($C_{23}H_{16}Cl_2FN_3O$, $[M+H]^+$). Anal. Calcd for ($C_{23}H_{16}Cl_2FN_3O$: C, 62.74; H, 3.66; N, 9.54; Found: C, 62.82; H, 3.50; N, 9.61%.

*4.3.17 (E)-3-(4-chlorophenyl)-1-phenyl-1H-pyrazole-4-carbaldehyde O-benzyl oxime (**4q**)*

White solid. Yield: 83%. Mp: 82-84 °C. ^{1}H NMR (300 MHz, DMSO-d_6): 5.13 (s, 2H); 7.32 (t, *J*=7.50Hz, 2H); 7.34-7.58 (m, 8H); 7.75 (d, *J*=8.40Hz, 2H); 7.94 (d, *J*=8.04Hz, 2H); 8.30 (s, 1H); 8.88 (s, 1H). MS (ESI): 388.4 ($C_{23}H_{18}ClN_3O$, $[M+H]^+$). Anal. Calcd

for $C_{23}H_{18}ClN_3O_2$: C, 71.22; H, 4.68; N, 10.83; Found: C, 71.29; H, 4.75; N, 11.02%.

*4.3.18 (E)-3-(4-chlorophenyl)-1-phenyl-1H-pyrazole-4-carbaldehyde O-(2-fluorobenzyl) oxime (**4r**)*

White solid. Yield: 65%. Mp: 75-77 °C. ^{1}H NMR(300 MHz, $CDCl_3$): 5.24 (s, 2H); 7.15 (m, 1H); 7.32 (t, *J*=7.50Hz, 2H); 7.40-7.51(m, 6H); 7.62 (d, *J*=7.11Hz, 2H); 7.75 (d, *J*=7.50Hz, 2H); 8.32 (s, 1H); 8.85 (s, 1H). MS (ESI): 406.2 ($C_{23}H_{17}ClFN_3O$, $[M+H]^+$). Anal. Calcd for $C_{23}H_{17}F_2N_3O$: C, 68.07; H, 4.22; N, 10.35; Found: C, 68.16; H, 4.07; N, 10.51%.

*4.3.19 (E)-3-(4-chlorophenyl)-1-phenyl-1H-pyrazole-4-carbaldehyde O-(2-chlorobenzyl) oxime (**4s**)*

White solid. Yield: 80%. Mp: 82-84 °C. ^{1}H NMR (300 MHz, DMSO-d_6): 5.22 (s, 2H); 7.35 (t, *J*=6.45Hz, 2H); 7.43 (m, 3H); 7.47-7.59 (m, 4H); 7.74 (d, *J*=8.61Hz, 2H); 7.94 (d, *J*=7.68Hz, 2H); 8.35 (s, 1H); 8.89 (s, 1H). MS (ESI): 423.6 ($C_{23}H_{17}Cl_2N_3O$, $[M+H]^+$). Anal. Calcd for $C_{23}H_{17}Cl_2N_3O$: C, 65.41; H, 4.06; N, 9.95; Found: C, 65.51; H, 4.23; N, 10.07%.

*4.3.20 (E)-3-(4-chlorophenyl)-1-phenyl-1H-pyrazole-4-carbaldehyde O-(2,4-dichlorobenzyl) oxime (**4t**)*

White solid. Yield: 85%. Mp: 147-149 °C. ^{1}H NMR (300 MHz, $CDCl_3$): 5.39 (s, 2H); 7.35-7.49 (m, 8H); 7.61 (d, *J*=8.61Hz, 2H); 7.74 (d, *J*=7.50Hz, 2H); 8.31 (s, 1H); 8.88 (s, 1H). MS (ESI): 457.4 ($C_{23}H_{16}Cl_3N_3O$, $[M+H]^+$). Anal. Calcd for $C_{23}H_{16}Cl_3N_3O$: C, 60.48; H, 3.53; N, 9.20; Found: C, 60.56; H, 3.61; N, 9.33%.

4.4 Crystal structure determination

Crystal structure determination of compound **4m** was carried out on a Bruker D8 VENTURE PHOTON equipped with graphite-monochromated MoKα (λ = 0.71073 Å) radiation. The structure was solved by direct methods and refined on F^2 by full-matrix least-squares methods using SHELX-97[26]. All the non-hydrogen atoms

were refined anisotropically. All the hydrogen atoms were placed in calculated positions and were assigned fixed isotropic thermal parameters at 1.2 times the equivalent isotropic U of the atoms to which they are attached and allowed to ride on their respective parent atoms.

4.5 Molecular docking

The PI3Kγ-LXX protein–ligand complex crystal structure (PDB code: 3L54) was used as the target structure in this approach. The molecular docking procedure was performed by using CDOCKER protocol for receptor-ligand interactions section of DS 3.1 (Discovery Studio 3.1, Accelrys, Inc., San Diego, CA)[32, 33].

4.6 Cellular activity

Cytotoxicities and inhibitory activities of compounds **4a-4t** on lymph node cells were evaluated, as described in previously study[22].

4.7 PI3Kγ inhibitory assay

Kinase assays of selected compounds (**4n**, **4p**, **4o**, **4r**, **4s**, **4b**, **4t**, **4g**, **4h** and **4e)** for IC_{50} value determinations with PI3Kγ (Minneapolis, MN) were carried out, as previously described[22].

4.8 IL-6 inhibitory assay

Mouse lymph node cells were incubated in DMEM media (Gibco) supplemented with 10% FBS, 100 U/mL penicillin, and 100 μg/mL streptomycin at 37 ^{o}C with 5% CO_2. Cells were pretreated with 5 μM of selected compounds **4n**, **4o**, **4p**, **4r** or vehicle control for 2 h, then treated with ConA (5 μg/mL) for 22 h. The culture media collected were centrifuged at 1000 rpm for 10 min. The levels of IL-6 in the media were determined by ELISA using mouse IL-6 ELISA Kits (BOSTER, USA) and strictly according to the manufacturer's instructions. Next, selected four compounds were tested with potent inhibitory activities against mRNA expression of IL-6 in ConA-simulated mouse lymph node cells using the RT-PCR assay.

Reference

[1] J.H. Cho, P.K. Gregersen, Genomics and the Multifactorial Nature of Human Autoimmune Disease, New Engl. J. Med., 365 (2011) 1612-1623.

[2] S.J. Chen, Y.L. Wang, H.C. Fan, W.T. Lo, C.C. Wang, H.K. Sytwu, Current Status of the Immunomodulation and Immunomediated Therapeutic Strategies for Multiple Sclerosis, Clin. Dev. Immunol., (2012).

[3] C.A. Dinarello, Anti-inflammatory Agents: Present and Future, Cell, 140 (2010) 935-950.

[4] P.Q. Eichacker, C. Parent, A. Kalil, C. Esposito, X. Cui, S.M. Banks, E.P. Gerstenberger, Y. Fitz, R.L. Danner, C. Natanson, Risk and the efficacy of antiinflammatory agents: retrospective and confirmatory studies of sepsis, Am. J. Respir. Crit. Care. Med., 166 (2002) 1197-1205.

[5] B. Vanhaesebroeck, S.J. Leevers, K. Ahmadi, J. Timms, R. Katso, P.C. Driscoll, R. Woscholski, P.J. Parker, M.D. Waterfield, Synthesis and function of 3-phosphorylated inositol lipids, Annu. Rev. Biochem., 70 (2001) 535-602.

[6] L.C. Cantley, The phosphoinositide 3-kinase pathway, Science, 296 (2002) 1655-1657.

[7] S. Ward, Y. Sotsios, J. Dowden, I. Bruce, P. Finan, Therapeutic potential of review phosphoinositide 3-kinase inhibitors, Chem. Biol., 10 (2003) 207-213.

[8] T.L. Yuan, L.C. Cantley, PI3K pathway alterations in cancer: variations on a theme, Oncogene, 27 (2008) 5497-5510.

[9] J.G. Foster, M.D. Blunt, E. Carter, S.G. Ward, Inhibition of PI3K Signaling Spurs New Therapeutic Opportunities in Inflammatory/Autoimmune Diseases and Hematological Malignancies, Pharmacol. Rev., 64 (2012) 1027-1054.

[10] M.P. Wymann, L. Pirola, Structure and function of phosphoinositide 3-kinases, Biochim. Biophys. Acta., 1436 (1998) 127-150.

[11] B. Vanhaesebroeck, J. Guillermet-Guibert, M. Graupera, B. Bilanges, The emerging mechanisms of isoform-specific PI3K signalling, Nat. Rev. Mol. Cell Biol., 11 (2010) 329-341.

[12] A.M. Condliffe, K. Davidson, K.E. Anderson, C.D. Ellson, T. Crabbe, K. Okkenhaug, B. Vanhaesebroeck, M. Turner, L. Webb, M.P. Wymann, E. Hirsch, T. Ruckle, M. Camps, C. Rommel, S.P. Jackson, E.R. Chilvers, L.R. Stephens, P.T. Hawkins, Sequential activation of class IB and class IA PI3K is important for the primed respiratory burst of human but not murine neutrophils, Blood, 106 (2005) 1432-1440.

[13] M.M. Al-Alwan, K. Okkenhaug, B. Vanhaesebroeck, J.S. Hayflick, A.J. Marshall, Requirement for phosphoinositide 3-kinase p110 delta signaling in B cell antigen receptor-mediated antigen presentation, J. Immunol., 178 (2007) 2328-2335.

[14] S.M. Johnson, H.M. Petrassi, S.K. Palaninathan, N.N. Mohamedmohaideen, H.E. Purkey, C. Nichols, K.P. Chiang, T. Walkup, J.C. Sacchettini, K.B. Sharpless, J.W. Kelly, Bisaryloxime ethers as potent inhibitors of transthyretin amyloid fibril formation, J. Med. Chem., 48 (2005) 1576-1587.

[15] D.P. Jindal, R. Chattopadhaya, S. Guleria, R. Gupta, Synthesis and antineoplastic activity of 2-alkylaminoethyl derivatives of various steroidal oximes, Eur. J. Med. Chem., 38 (2003) 1025-1034.

[16] A. Balsamo, M.C. Breschi, M. Chini, P. Domiano, G. Giannaccini, A. Lucacchini, B. Macchia, M. Macchia, C. Manera, A. Martinelli, C. Martini, E. Martinotti, P. Nieri, A. Rossello, CONFORMATIONALLY RESTRAINED BETA-BLOCKING OXIME ETHERS - SYNTHESIS AND BETA-ADRENERGIC PROPERTIES OF DIASTEREOISOMERIC ANTI AND SYN 2-(5'-ISOXAZOLIDINYL)-ETHANOLAMINES, Eur. J. Med. Chem., 27

(1992) 751-764.
[17] R.A. Chapman, C.R. Harris, Determination of residues of methomyl and oxamyl and their oximes in crops by gas-liquid chromatography of oxime trimethylsilyl ethers, J. Chrom., 171 (1979) 249-262.
[18] C. Ramalingan, Y.T. Park, S. Kabilan, Synthesis, stereochemistry, and antimicrobial evaluation of substituted piperidin-4-one oxime ethers, Eur. J. Med. Chem., 41 (2006) 683-696.
[19] A.P. Keche, G.D. Hatnapure, R.H. Tale, A.H. Rodge, V.M. Kamble, Synthesis, anti-inflammatory and antimicrobial evaluation of novel 1-acetyl-3,5-diaryl-4,5-dihydro (1H) pyrazole derivatives bearing urea, thiourea and sulfonamide moieties, Bioorg. Med. Chem. Lett., 22 (2012) 6611-6615.
[20] K.S. Girisha, B. Kalluraya, V. Narayana, Padmashree, Synthesis and pharmacological study of 1-acetyl/propyl-3-aryl-5-(5-chloro-3-methyl-1-phenyl-1H-pyrazol-4-yl)-2- pyrazoline, Eur. J. Med. Chem., 45 (2010) 4640-4644.
[21] E. Bansal, V.K. Srivastava, A. Kumar, Synthesis and anti-inflammatory activity of 1-acetyl-5-substitute daryl-3-(beta-aminonapthyl)-2-pyrazolines and beta-(substituted aminoethyl) amidonaphthalenes, Eur. J. Med. Chem., 36 (2001) 81-92.
[22] J.-F. Tang, X.-H. Lv, X.-L. Wang, J. Sun, Y.-B. Zhang, Y.-S. Yang, H.-B. Gong, H.-L. Zhu, Design, synthesis, biological evaluation and molecular modeling of novel 1,3,4-oxadiazole derivatives based on Vanillic acid as potential immunosuppressive agents, Bioorg. Med. Chem., 20 (2012) 4226-4236.
[23] R. Yan, Z.-M. Zhang, X.-Y. Fang, Y. Hu, H.-L. Zhu, Synthesis, molecular docking and biological evaluation of 1,3,4-oxadiazole derivatives as potential immunosuppressive agents, Bioorg. Med. Chem., 20 (2012) 1373-1379.
[24] Z.-M. Zhang, X.-W. Zhang, Z.-Z. Zhao, R. Yan, R. Xu, H.-B. Gong, H.-L. Zhu, Synthesis, biological evaluation and molecular docking studies of 1,3,4-oxadiazole derivatives as potential immunosuppressive agents, Bioorg. Med. Chem., 20 (2012) 3359-3367.
[25] T.D. Penning, J.J. Talley, S.R. Bertenshaw, J.S. Carter, P.W. Collins, S. Docter, M.J. Graneto, L.F. Lee, J.W. Malecha, J.M. Miyashiro, R.S. Rogers, D.J. Rogier, S.S. Yu, G.D. Anderson, E.G. Burton, J.N. Cogburn, S.A. Gregory, C.M. Koboldt, W.E. Perkins, K. Seibert, A.W. Veenhuizen, Y.Y. Zhang, P.C. Isakson, Synthesis and biological evaluation of the 1,5-diarylpyrazole class of cyclooxygenase-2 inhibitors: Identification of 4- 5-(4-methylphenyl)-3-(trifluoromethyl)-1H-pyrazol-1-yl benzenesulfona mide (SC-58635, Celecoxib), J. Med. Chem., 40 (1997) 1347-1365.
[26] G.M. Sheldrick, SHELXTL-97, Program for Crystal Structure Solution and Refinement, University of Göttingen, Göttingen, Germany, 1997.
[27] C.J. Vlahos, W.F. Matter, K.Y. Hui, R.F. Brown, A specific inhibitor of phosphatidylinositol 3-kinase, 2-(4-morpholinyl)-8-phenyl-4H-1-benzopyran-4-one (LY294002), J. Biol. Chem., 269 (1994) 5241-5248.
[28] H. Tilg, C.A. Dinarello, J.W. Mier, IL-6 and APPs: anti-inflammatory and immunosuppressive mediators, Immunol. Today, 18 (1997) 428-432.
[29] S.M. Opal, V.A. DePalo, Anti-inflammatory cytokines, Chest, 117 (2000) 1162-1172.
[30] K. Ishihara, T. Hirano, IL-6 in autoimmune disease and chronic inflammatory proliferative disease, Cytokine Growth Factor Rev., 13 (2002) 357-368.
[31] C.H. Tang, D.Y. Lu, R.S. Yang, H.Y. Tsai, M.C. Kao, W.M. Fu, Y.F. Chen, Leptin-induced IL-6 production is mediated by leptin receptor, insulin receptor substrate-1, phosphatidylinositol 3-kinase, Akt, NF-kappa B, and p300 pathway in microglia, J. Immunol., 179 (2007) 1292-1302.
[32] Discovery Studio 3.1, Accelrys Software Inc., San Diego, 2011.
[33] G. Wu, D.H. Robertson, C.L. Brooks, M. Vieth, Detailed analysis of grid-based molecular docking: A case study of CDOCKER—A CHARMm-based MD docking algorithm, J. Comput. Chem., 24 (2003)

1549-1562.

Table 1. Crystallographic and Experimental Data for compound **4m.**

Compound	**4m**
Formula	$C_{23}H_{18}FN_3O$
Crystal size(mm)	0.31×0.23×0.17
MW(g mol^{-1})	371.40
Crystal system	Triclinic
α (°)	96.327(9)
β(°)	96.542(10)
γ(°)	108.859(7)
a(Å)	8.272(6)
b(Å)	10.477(8)
c(Å)	23.85(2)
V($Å^3$)	1919(3)
Z	4
θ limits(°)	2.13≤θ≤24.74
hkl limits	-16 ≤h≤16, -13≤k≤14, -13 ≤l≤12
F(000)	776
Data/restraints/parameters	6442/1/505
Absorption coefficient(mm^{-1})	0.087
Reflections collected	12975
Independent reflections	6442 [R_{int}= 0.0392]
R_1/ wR_2 [I>2&Gs(I)]	0.0596/ 0.1489
R_1/ wR_2 (all data)	0.1408/ 0.1966
Goodness-of-fit on F^2	1.005

Table 2. Cytotoxicities and inhibitory activities of compounds **4a–4t** on lymph node cells.

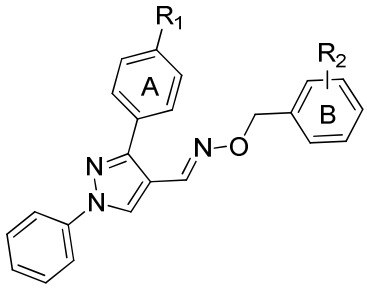

Compound	R_1	R_2	CC_{50}±SD（μM）	IC_{50}±SD（μM）	SI
4a	H	H	376.14±23.15	18.33±5.64	20.52
4b	H	2-F	434.52±26.75	10.36±0.39	41.94
4c	H	2-Cl	325.64±23.71	19.10±0.75	17.05
4d	H	2,4-Cl	276.73±36.34	16.75±0.68	16.52
4e	CH_3	H	328.59±19.27	40.57±2.45	8.10
4f	CH_3	2-F	382.56±27.65	28.00±3.72	13.66
4g	CH_3	2-Cl	275.19±27.35	34.58±5.43	7.96
4h	CH_3	2,4-Cl	228.68±19.36	38.30±7.56	5.97
4i	OCH_3	H	348.58±21.63	26.29±0.78	13.26
4j	OCH_3	2-F	374.87±16.39	20.22±1.87	18.54
4k	OCH_3	2-Cl	289.51±25.64	20.16±1.76	14.36
4l	OCH_3	2,4-Cl	212.08±18.35	27.23±3.64	7.79
4m	F	H	319.43±36.74	17.57±1.67	18.18
4n	F	2-F	259.12±22.72	1.18±0.26	219.59
4o	F	2-Cl	296.89±27.45	2.74±0.24	108.35
4p	F	2,4-Cl	375.47±27.62	7.22±1.18	52.00
4q	Cl	H	333.36±28.34	18.45±0.76	18.07
4r	Cl	2-F	362.28±25.68	8.03±0.25	45.12
4s	Cl	2-Cl	323.71±23.67	9.08±0.06	35.65
4t	Cl	2,4-Cl	265.78±38.32	10.76±0.17	24.70
	CsA		178.26±27.87	0.57±0.01	312.73

Table 3. PI3Kγ inhibitory activity of the selected compounds

compound	IC_{50} PI3Kγ (μM)
4n	0.28
4p	1.26
4o	3.12
4r	12.36
4s	13.78
4b	6.57
4t	9.36
4g	21.45
4h	>25
4e	>25
LY294002	7.2

Figure caption:

Figure 1. The structure of compounds A–C.

Figure 2. Title compounds.

Figure 3. Docking model of compound **4p** with PI3Kγ. It is nicely bound to the PI3Kγ via three H-bonds (Ser806 - F: 2.10 Å, 139.0^{o}, Lys890 - O: 2.27 Å, 108.5^{o}, Lys890 - N19: 2.33 Å, 126.8^{o}) and a Pi-cation interaction (3.2 Å).

Figure 4. The molecular structure of **4m** showing 30% probability displacement ellipsoids.

Figure 5. (a) Selected compounds inhibited ConA-induced IL-6 secretion in Mouse lymph node cells. (b) The RT-PCR results of selected compounds (5 M) inhibit mRNA expression of IL-6.

Scheme 1. General synthesis of compounds 4a–4t. R_1=H, CH_3, OCH_3, F, Cl; R_2=H, 2-F, 2-Cl, 2, 4-Cl. i：ethanol, 50-60 ^{o}C, 3h；ii：DMF, $POCl_3$, 50-60 ^{o}C, 5h; iii：sub-benzylhydroxyamine hydrochloride, ethanol, NaOAc, 30 ^{o}C, 3h

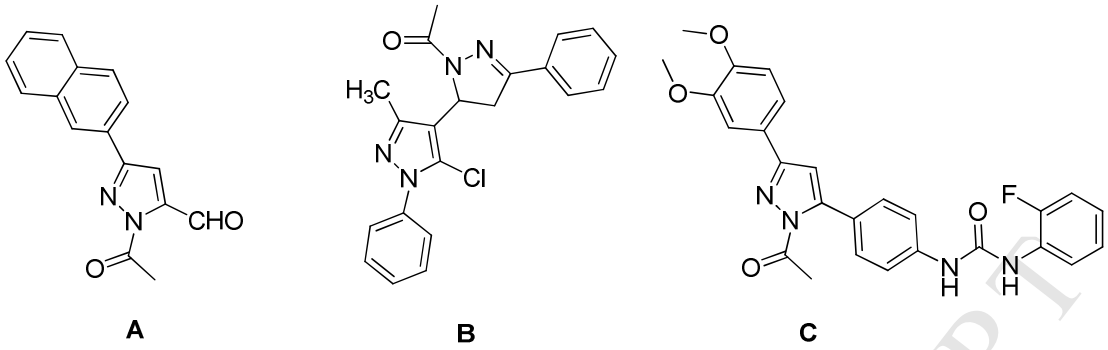

Figure 1.

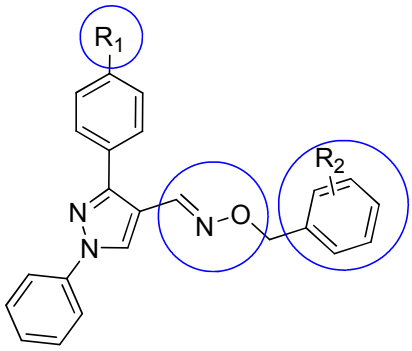

4a-4t

Figure 2.

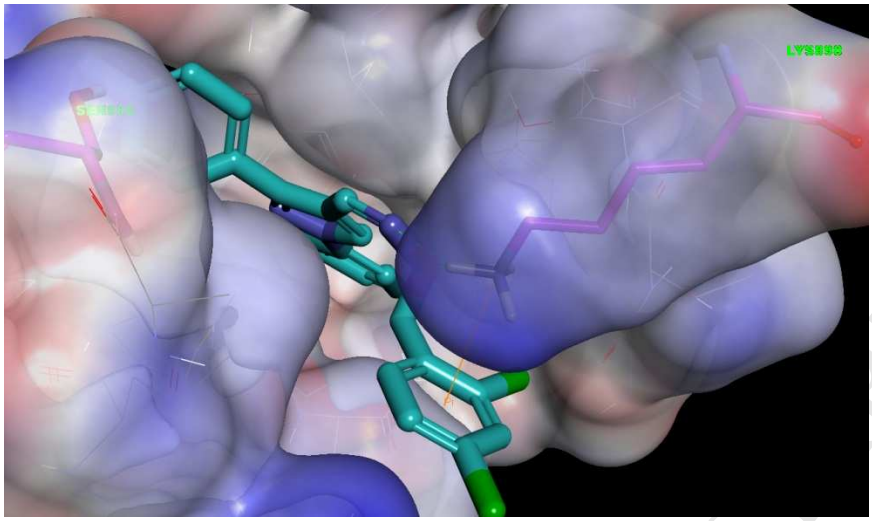

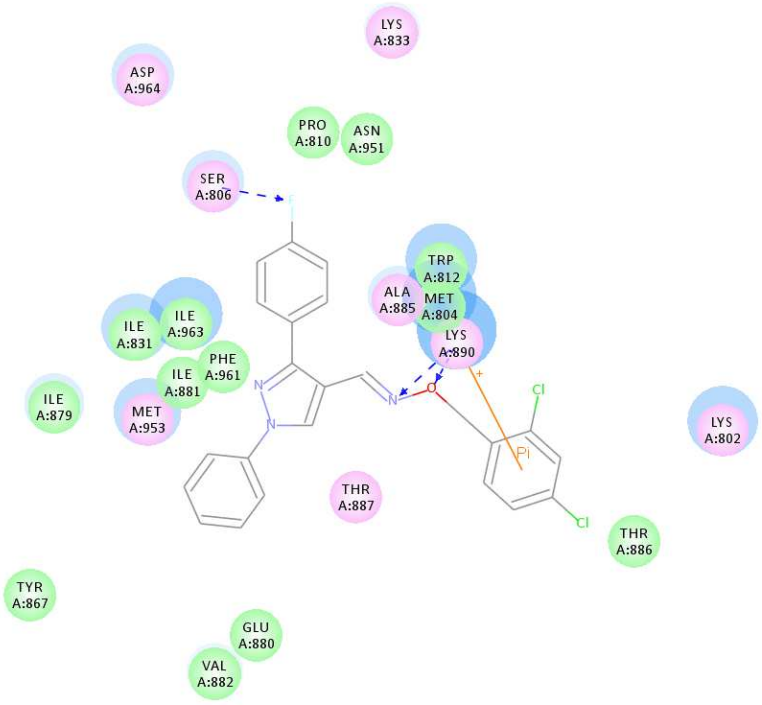
LYS A:833
ASP A:964
PRO A:810
ASN A:951
SER A:806
TRP A:812
ALA A:885
MET A:804
LYS A:890
ILE A:831
ILE A:963
PHE A:961
ILE A:881
ILE A:879
MET A:953
Cl
LYS A:802
Pi
THR A:887
Cl
THR A:886
TYR A:867
GLU A:880
VAL A:882

Figure 3.

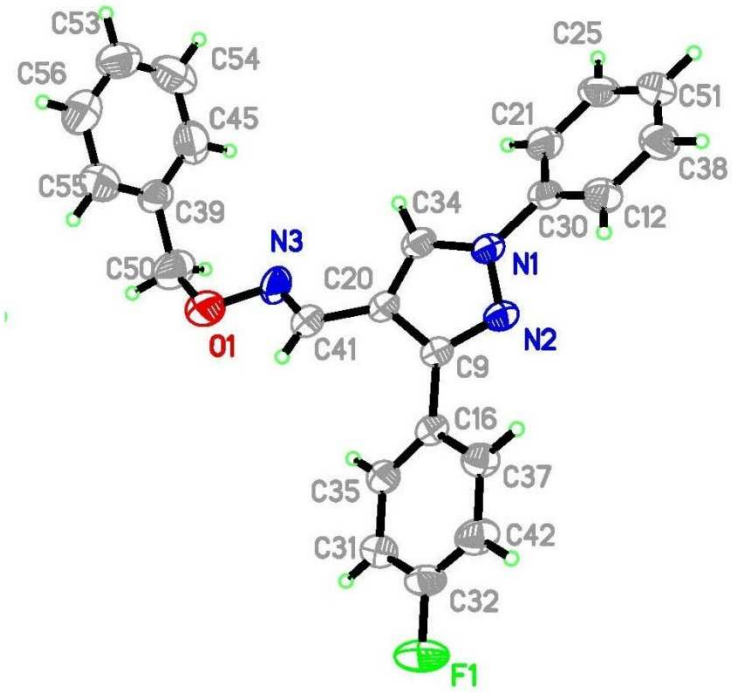

Figure 4.

(A)

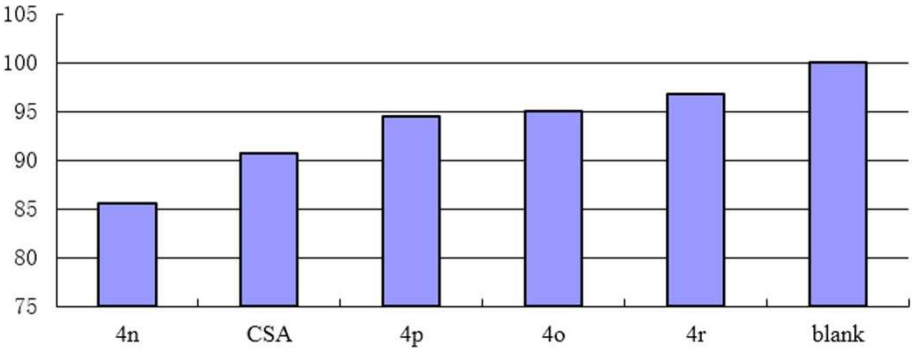

(B)

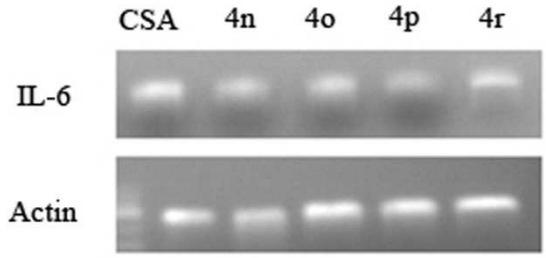

Figure 5.

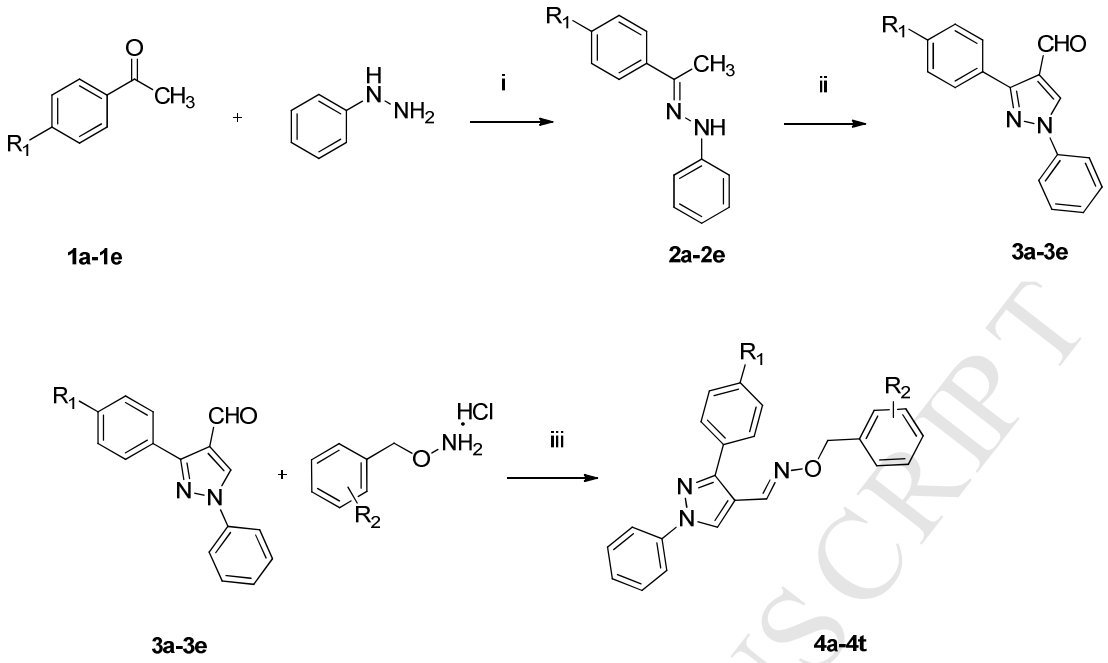

Scheme 1.

> A series of novel pyrazole O-benzyl oxime derivatives were synthesized.

> **4n** exhibited the most potent immunosuppressive activity.

> **4n** exhibited significantly PI3Kγ inhibitory activity.

Representative ^{1}H and ^{13}C NMR spectra :

*(E)-3-(4-fluorophenyl)-1-phenyl-1H-pyrazole-4-carbaldehyde O-benzyl oxime (**4m**)*

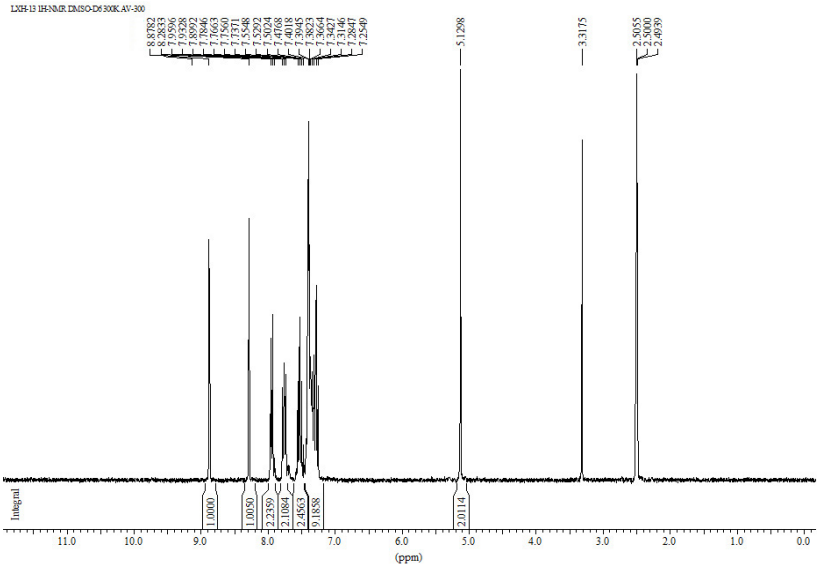

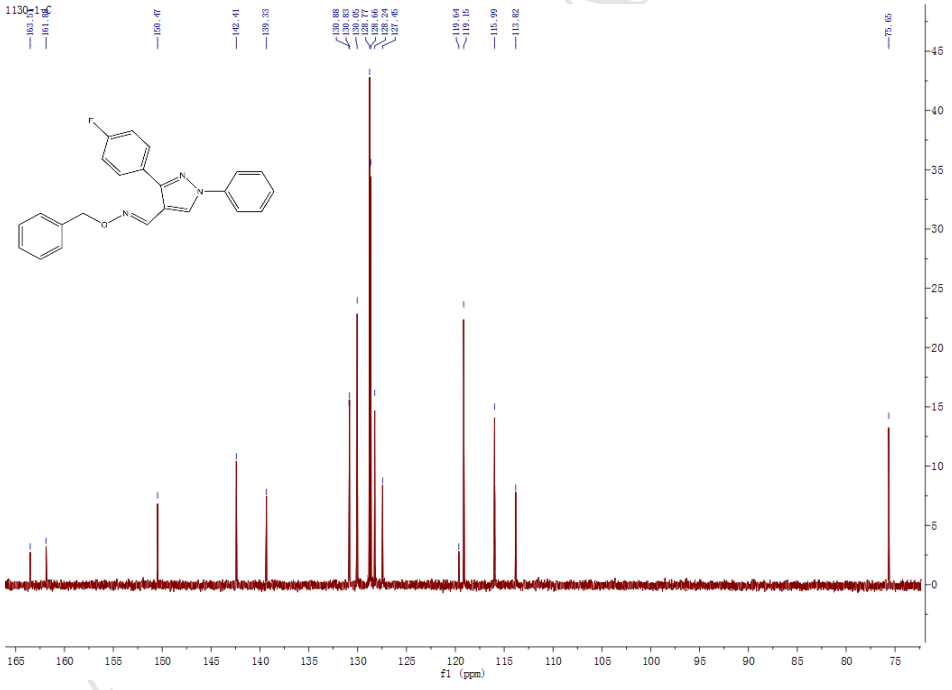

*(E)-3-(4-fluorophenyl)-1-phenyl-1H-pyrazole-4-carbaldehyde O-(2-fluorobenzyl) oxime (**4n**)*

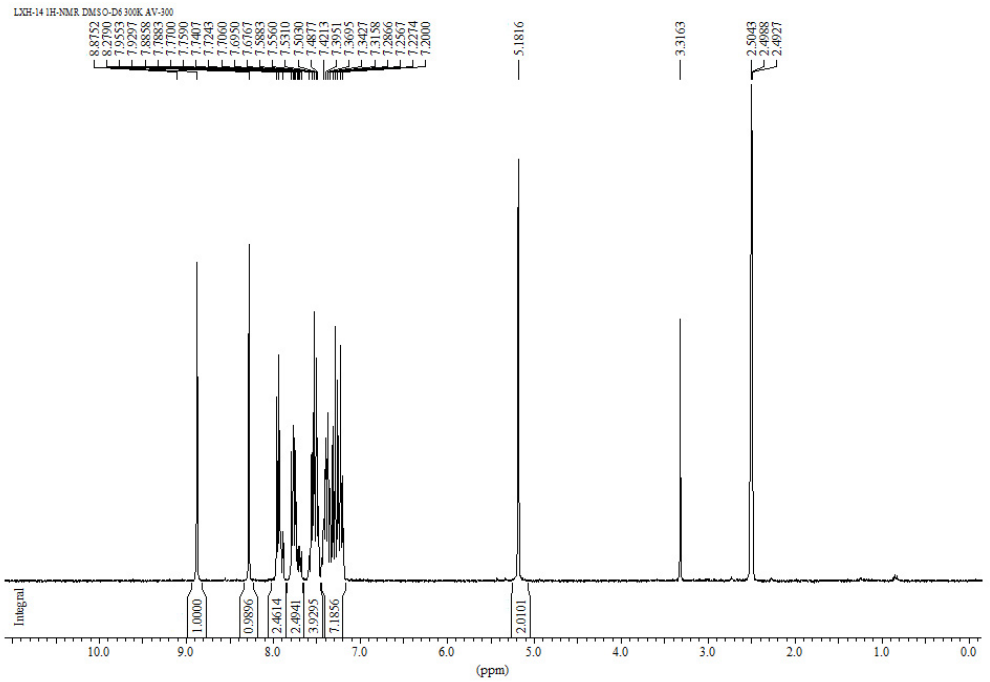

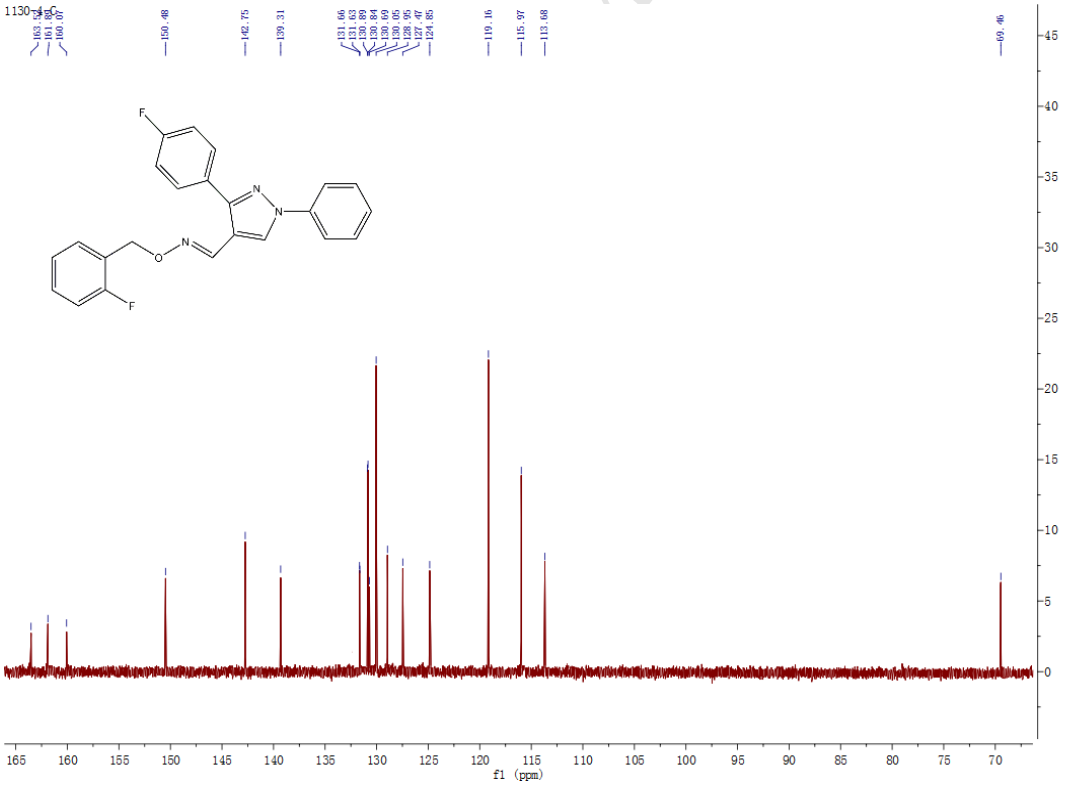

*(E)-3-(4-fluorophenyl)-1-phenyl-1H-pyrazole-4-carbaldehyde O-(2-chlorobenzyl) oxime (**4o**)*

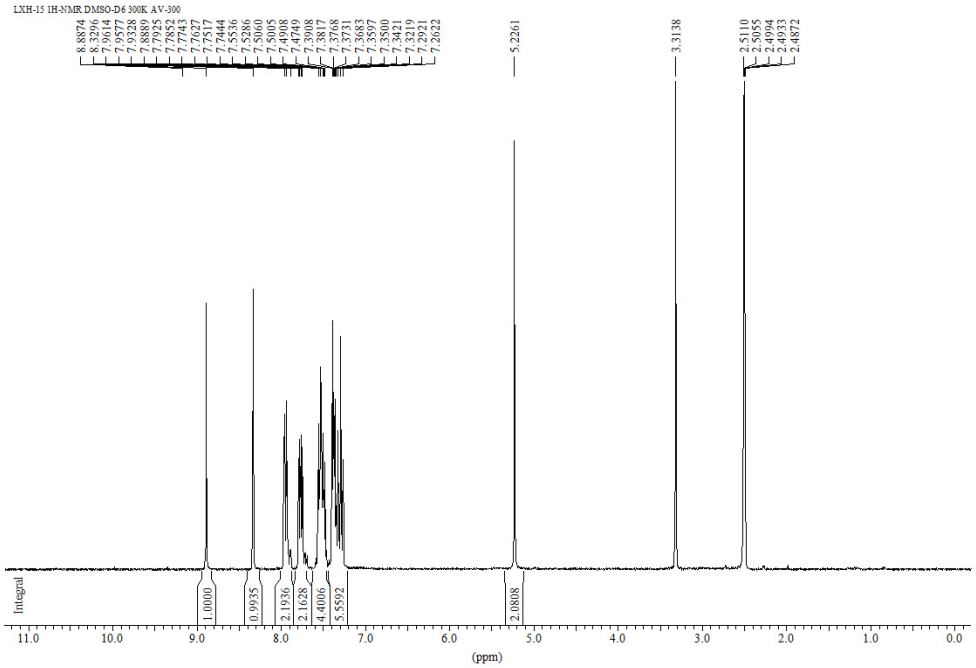
LXH-15 1H-NMR DMSO-D6 300K AV-300
8.8874
8.3796
7.9614
7.9577
7.9328
7.8889
7.7925
7.7852
7.7743
7.7627
7.7517
7.7444
7.5536
7.5286
7.5060
7.5005
7.4908
7.4749
7.3908
7.3817
7.3768
7.3731
7.3683
7.3597
7.3500
7.3421
7.3219
7.2921
7.2622
5.2261
3.3138
2.5110
2.5055
2.4994
2.4933
2.4872
Integral
1.0000
0.9935
2.1936
2.1628
4.4006
5.5592
2.0808
(ppm)

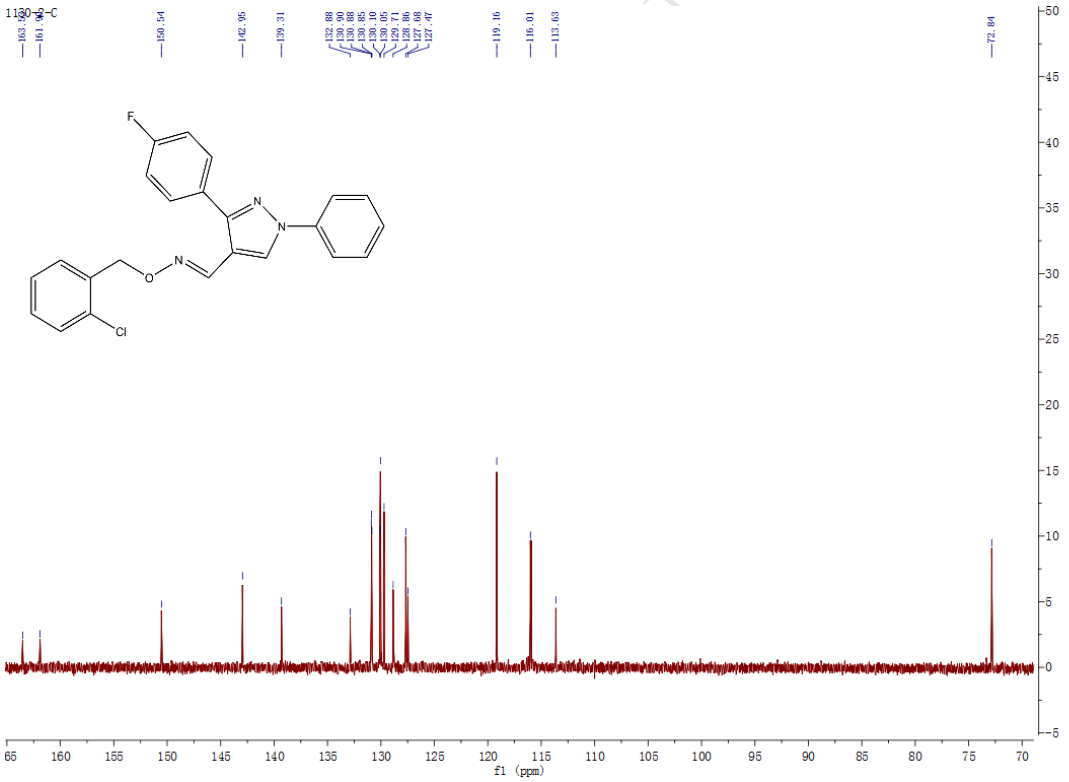
1130-2-C
163.58
161.94
150.54
142.95
139.31
132.88
130.99
130.88
130.85
130.10
130.05
129.71
128.86
127.68
127.47
119.16
116.01
113.63
72.84
F
N
N
O
N
Cl
f1 (ppm)